



An experimental aluminum-fueled power plant

M.S. Vlaskin*, E.I. Shkolnikov, A.V. Bersh, A.Z. Zhuk, A.V. Lisicyn, A.I. Sorokovikov, Yu.V. Pankina

The Joint Institute for High Temperatures, Ijorskaya st. 13/2, 125412 Moscow, Russia

ARTICLE INFO

Article history:

Received 31 January 2011

Received in revised form 23 May 2011

Accepted 3 June 2011

Available online 13 June 2011

Keywords:

Aluminum

Water

Hydrogen

Fuel cell

Power plant

Co-generation

ABSTRACT

An experimental co-generation power plant (CGPP-10) using aluminum micron powder (with average particle size up to 70 μm) as primary fuel and water as primary oxidant was developed and tested. Power plant can work in autonomous (unconnected from industrial network) nonstop regime producing hydrogen, electrical energy and heat. One of the key components of experimental plant is aluminum–water high-pressure reactor projected for hydrogen production rate of $\sim 10 \text{ nm}^3 \text{ h}^{-1}$. Hydrogen from the reactor goes through condenser and dehumidifier and with -25°C dew-point temperature enters into the air–hydrogen fuel cell 16 kW–battery. From 1 kg of aluminum the experimental plant produces 1 kWh of electrical energy and 5–7 kWh of heat. Power consumer gets about 10 kW of electrical power. Plant electrical and total efficiencies are 12% and 72%, respectively.

© 2011 Elsevier B.V. All rights reserved.

1. Introduction

Aluminum has been proposed for the role of perspective non-organic energy storage mater by a number of researchers [1–9]. Potentially high level of aluminum integration in future energy economy is mainly bound with high content of aluminum in the earth's crust [10], safety and moderate cost of aluminum storage and transportation [11], as well as possible regeneration of such energy carrier.

Exothermic process of aluminum oxidation in aqueous solutions with the production of hydrogen as intermediate fuel proved to be one of the effective technologies that convert aluminum chemical energy into useful energy (electrical or thermal) [2,7,12–17]. Recently developed method of aluminum micron powder oxidation in high-temperature water steam [12,13] allowed applying pure (without alkali and any other chemical activators) water as oxidant. Kinetics of aluminum micron powders oxidation in high-temperature boiling water was studied in [18]. It was established that aluminum powders with average particle size from 4 to 70 μm , which are produced in industrial scale, were intensively oxidized

within special reactor under about 300°C and 10 MPa water steam; the reaction time was several tens of seconds.

Further development of power plant based on “aluminum–water” reactor as high-pressure steam–hydrogen generator was based on the results of kinetic experiments and a number of designing investigations. One of such calculations was presented in [19]. It was devoted for thermodynamics of nonstop reactor operation. Reactor thermo- and gas-dynamic parameters estimation and optimization was carried out in that work, an optimum parameter field (composed of reactor temperature, pressure, volume and others) in the view of thermodynamic effectiveness was determined.

Based on the results of [18,19] and other designing investigations an experimental co-generation power plant CGPP-10 was developed. It consumes aluminum micron powder as primary fuel and pure water as primary oxidant. Hydrogen, which is produced within aluminum–water reactor, is used as secondary fuel for electrical energy generation. “10” in power plant label means nominal hydrogen generation rate in “ $\text{nm}^3 \text{ h}^{-1}$ ”. CGPP-10 outputs useful electrical energy and heat. If it is necessary, CGPP-10 can produce hydrogen as end product.

In present work CGPP-10 structure, operation principle and operation features are considered. One of the primary purposes of experimental activities was CGPP-10 nonstop run organization. It was attained and so the results of nonstop test are presented in this work. Both each CGPP-10 component separately and experimental plant wholly are studied. Following the results of experiment main CGPP-10 technical specifications and energy indexes are examined. Thermodynamic and economic analyses for CGPP-10 are also estimated.

Abbreviations: RB, reactor block; ECG, electrochemical generator; AHFC, air–hydrogen fuel cell; EETDS, energy transformation and distribution system; FH, fan heater; HT, hydrogen tank; ACMS, automated control and management system; DHPP, dosage high-pressure pump; T_i , temperature sensor; P_i , pressure sensor; L_i , liquidometer; CV, cutoff valve; OWV, one-way valve; VI, voltage inverter; LABB, lead-acid batteries block; BC, battery charger; FS, feeder switchboard; BL, ballast load.

* Corresponding author. Tel.: +7 495 4851055; fax: +7 495 4851055.

E-mail address: vlaskin@inbox.ru (M.S. Vlaskin).

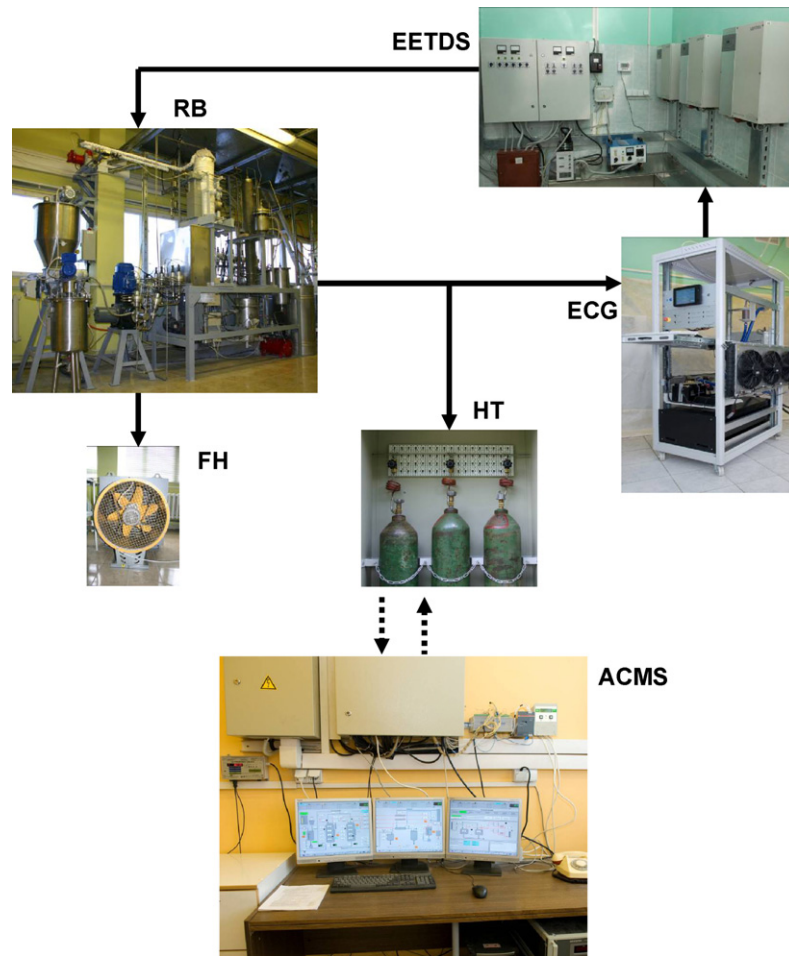


Fig. 1. CGPP-10 main components. RB – reactor block, HT – hydrogen tank, ECG – electrochemical generator, FH – fan heater, EETDS – electrical energy transformation and distribution system, and ACMS – automated control and management system.

2. Experimental plant

Experimental plant general components are shown in Fig. 1. The crucial unit of CGPP-10 is the reactor block (RB) where in accordance with the developed method of aluminum micron powder oxidation the nonstop process of hydrogen and heat generation was realized. For hydrogen utilization an electrochemical generator (ECG) based on the air-hydrogen fuel cells (AHFCs) was chosen. Electrical energy produced by AHFC battery is directed to the electrical energy transformation and distribution system (EETDS). EETDS realizes CGPP-10 power supply switch from industrial network to ECG (and back) providing autonomous, non-networked, operation of whole experimental complex. Thermal energy produced by RB is transformed into the useful heat warming up the room by means of fan heater (FH). For ECG trouble-free performance the CGPP-10 involves hydrogen tank (HT), which smoothes the electrical energy consumption irregularity and in case of zero load stores the secondary fuel. Experimental plant is remotely managed by operator from operating room through the automated control and management system (ACMS).

2.1. Reactor block

RB in-life view and its schematic diagram are shown in Fig. 2a and b, respectively. Nonstop hydrogen and heat generation in RB is based on nonstop initial reagents (water and aluminum powder) supply to reactor and simultaneous nonstop oxidation products

removing from reactor. Aluminum powder is entered into the reactor in the form of aluminum–water mixture with fixed value of water to aluminum mass ratio. Mixture is prepared within mixing tank. Aluminum into the mixing tank goes from aluminum powder storage bunker by means of dosage screw; water goes from distilled water tank by means of dosage pump. During the experiment the mixture level in mixing tank is kept within fixed interval and it is controlled by liquidometer. Necessary water to aluminum mass ratio in the mixture is achieved due to the preliminary motor frequency adjustment of dosage devices.

From mixing tank to reactor the mixture is entered with the help of dosage high-pressure pump (DHPP). The products of aluminum–water reaction are removed from the reactor both from the top and from the bottom. From the top of the reactor mainly gaseous phase of oxidation products (hydrogen and water steam mixture) is removed, from the bottom—aluminum hydroxide and water in condensed state. Aluminum powder is fully oxidized within the reactor, because condensed phase necessary volume is always maintained in the bottom of reactor. Condensed phase volume is controlled by contactless level sensor, which governs the removing of oxidation products from the bottom of reactor. From the top of the reactor the products are removed through the controllable valve with variable cross-section.

Hydrogen and water steam mixture goes from the reactor into the heat exchanger, where it is cooled by circuit water. Thermal energy, which is transferred to the heat exchanger, is spent on circuit water heating and room warming. Hydrogen and condensed

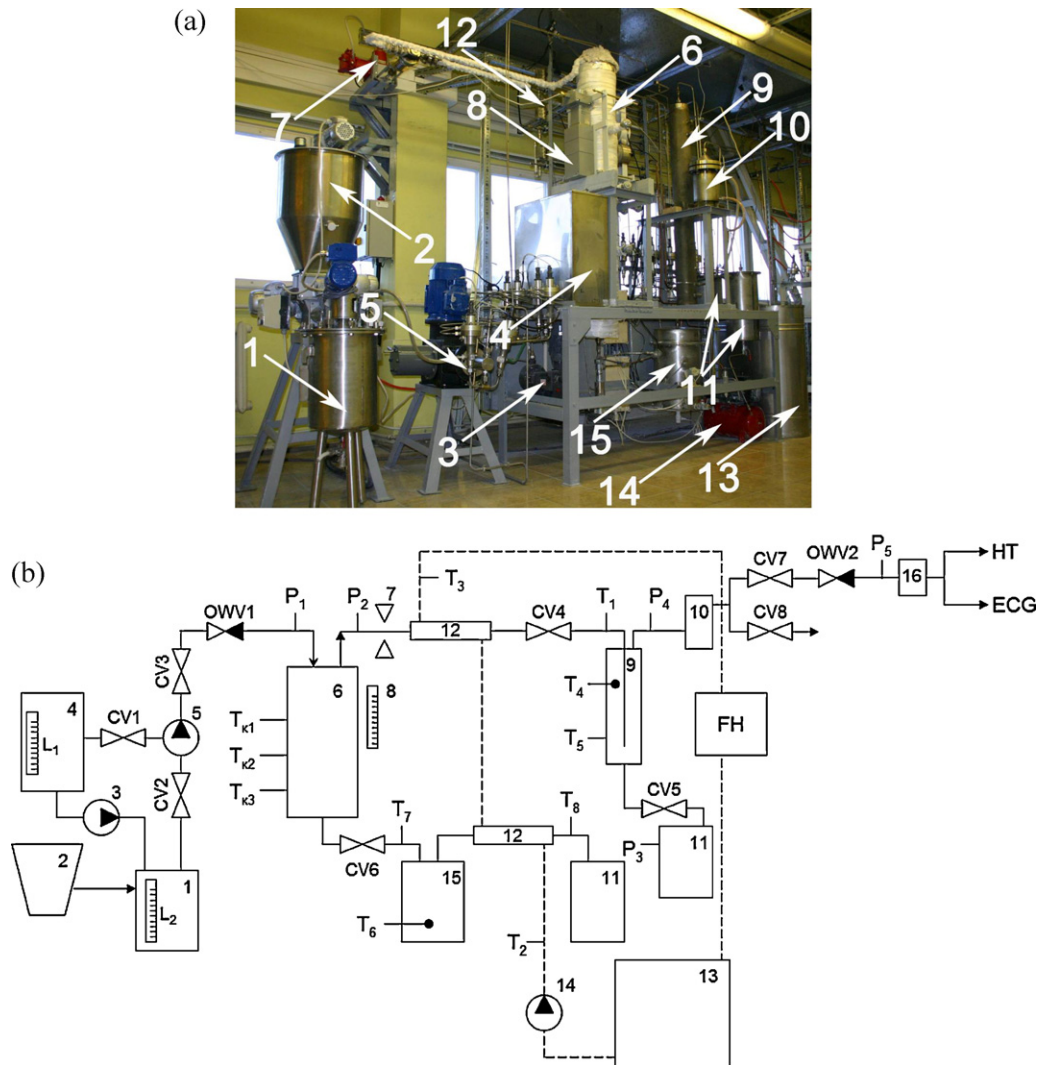


Fig. 2. (a) RB in-life view and (b) RB schematic diagram. 1 – mixing tank, 2 – aluminum powder storage and dosage system, 3 – water dosage pump, 4 – distilled water tank, 5 – dosage high-pressure pump (DHPP), 6 – reactor, 7 – variable cross-section valve, 8 – contactless level sensor, 9 – condenser, 10 – hydrogen dehumidifier, 11 – hotwells, 12 – heat exchanger, 13 – circuit water tank, 14 – circuit water pump, 15 – oxidation products receiving tank, 16 – hydrogen humidity sensor. $T_{k1} \dots T_{k3}$, $T_1 \dots T_8$ – temperature sensors, $P_1 \dots P_5$ – pressure sensors, L_1 , L_2 – liquidometers. CV1...CV8 – cutoff valves and OWV1, OWV2 – one-way valves.

water go from the heat exchanger into the condenser. From the condenser the hydrogen goes into the dehumidifier and then comes into ECG and HT, while water is periodically removed from the condenser into the hotwell. Condensed products are removed from the reactor into the oxidation products receiving tank. Reaction products pass through the narrow orifice and due to the throttling the water steam is produced within the oxidation products receiving tank. This steam goes into the heat exchanger. After the heat exchanger the condensed water goes into the respective hotwell. All hotwell-collected water goes back to the distilled water tank.

2.2. Electrochemical generator

Main component of ECG is AHFC battery HyPM HD16 manufactured by Hydrogenics. ECG has own control and management system and cooling circuit module (Fig. 3). ECG technical specifications are shown in Table 1.

ECG start and stop are carried out with the help of its own control and management system. ECG consumes hydrogen and generates DC-electrical energy and low-grade heat. Electrical energy from ECG goes to EETDS.

2.3. Electrical energy transformation and distribution system

EETDS consists of voltage inverter (VI) manufactured by Xantrex, lead-acid batteries block (LABB), battery charger (BC) and four-step ballast loads BL1 and BL2 (Fig. 4). BL1 imitates DC-power consumer, BL2 – AC-power consumer. Steps in both BL1 and BL2 are parallel-connected. BL1 ohmic resistances are 3, 2, 1.3 and 1 Ω . Each BL2 step consumes 3 kW AC-power. BL1 is powered directly by ECG or LABB. BL2 is powered through VI, which transforms the ECG DC-voltage into the three-phase AC-voltage.

All CGPP-10 auxiliary equipment (DHPP, dosage devices, mixing tank, etc.) is connected up to common feeder switchboard (FS). FS and BC are attached to VI.

Table 1
ECG technical specifications.

Parameter	Unit	Value
Power	kW	16.5
Output voltage range	V	40–80
Output current range	A	0–350
Number of AHFCs	pcs	80
Peak electrical efficiency	%	56

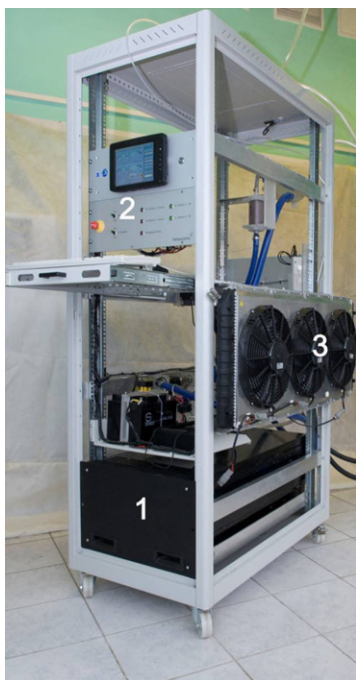


Fig. 3. ECG. 1 – AHFC battery, 2 – control and management system, and 3 – cooling circuit module.

CGPP-10 autonomous starting should be realized by means of LABB, which should feed the auxiliary equipment until the hydrogen is produced. The use of LABB on power plant board for its autonomous starting allows excluding on-board hydrogen keeping during the power plant standby mode.

2.4. Experimental procedure

Here the common CGPP-10 experimental procedure is presented. It shows the sequence of operations and allowed ranges of operating parameters.

Experimental procedure involves three main stages: pre-starting operations, operating mode and putting into initial state. During the operating mode CGPP-10 is managed through ACMS in accordance with early-developed and programmed algorithm, i.e. all operations are automated. On the contrary, the execution of pre-starting operations and putting into initial state requires direct operator participation.

Pre-starting stage prepares CGPP-10 components for operating mode and includes the following operations: from LABB to VI power supply initialization, from VI to FS power supply initialization, ACMS and ECG control and management system loading, hydrogen pipelines blowing by nitrogen, preliminary reactor heat-

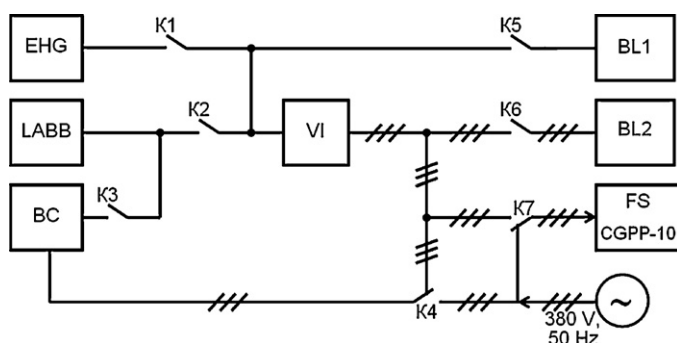


Fig. 4. EETDS electrical scheme.

ing, first portion of aluminum–water mixture preparation within mixing tank, hand valves opening. Three standard hydrogen balloons each 40 l are attached to RB. In experiments balloons are initially squeezed by hydrogen with initial pressure from the interval of 1–4 MPa. During the pre-starting operations stage CGPP-10 auxiliary equipment is powered by industrial network (380 V and 50 Hz). ACMS and ECG control and management system data are uninterruptedly written on respective hard disk drives all time of experiment.

Reactor is heated to 300 °C or more by means of ohmic heater installed on reactor surface. During the heating the reactor is preliminary filled by water. Water is taken from the distilled water tank (Fig. 2b). At the end of reactor heating the saturated wet steam of water is created, water steam pressure exceeds 8 MPa.

CGPP-10 primary fuel is aluminum powder with the average particle size up to 70 μm. Mixing tank is filled by aluminum powder and distilled water by means of aluminum powder dosage screw and water dosage pump respectively. Motor frequency regulators of respective dosage devices are preliminary adjusted to provide the water to aluminum mass ratio from the interval of 7–9.

When all pre-starting operations are completed, operator pushes the start button on ACMS monitor (Fig. 1) and so operating mode starts. During this mode all operations (excepting ECG start and stop) are automated. Start button clicking switches the FS power supply from industrial network to LABB through VI (Fig. 4). The safety of this switching is provided by uninterruptible power supply battery, which is included into FS.

During the operating mode DHPP uninterruptedly injects the aluminum–water mixture into the reactor. Due to chemical reaction between aluminum powder and water steam the reactor pressure increases and when it reaches the fixed value CV4 opens. Always when CV4 is opened the circuit water pump is turned on. Produced hydrogen and water steam mixture goes from reactor through open CV4 into the heat exchanger (Fig. 2b). When CV4 is opened the reactor pressure is maintained with the help of variable cross-section valve. Allowed reactor pressure range lies in the interval of 10–20 MPa. DHPP supplies the reactor with aluminum at the rate of 2.3–3 g s⁻¹ that provides hydrogen generation rate over 10 nm³ h⁻¹. CV4 does not close during the operating mode.

When reactor is filled by condensed products up to fixed level, which is controlled by contactless level sensor, CV6 opens for a short period and so oxidation products are partially removed from the reactor to the oxidation products receiving tank (Fig. 2b). In nominal reactor conditions the volume of condensed products occupies not less than 60% from total reactor volume (7.5 l). The maintenance of such level guarantees that aluminum stays inside the reactor space under high-temperature boiling water conditions for not less than 200 s that provides in the long run ~100% degree of aluminum conversion [18].

During first minutes of operating mode the initial hydrogen purge is carried out. Hydrogen purges the condenser and dehumidifier through CV8 (Fig. 2b). Then, when condenser pressure reaches the fixed value, CV7 opens and hydrogen from reactor comes into HT and ECG.

When CV7 opens, operator starts ECG by clicking the respective start button on the ECG monitor (Fig. 3). ECG open circuit voltage nears to 80 V while VI is not recommended (by its manufacturer) to be energized by voltage over 70 V. Therefore, ECG is loaded in the following way: at first two steps of BL1 are attached to ECG that decreases the ECG output voltage, then ECG joins to the LABB for parallel CGPP-10 auxiliary feeding and finally ECG is loaded on two unused steps of BL1 (Fig. 4). Such loading sequence provides the reliable ECG and VI cooperation. Since experimental plant electric system involves at one time nonsynchronous three-phase and one-phase AC-motors and, moreover, DHPP creates strong current

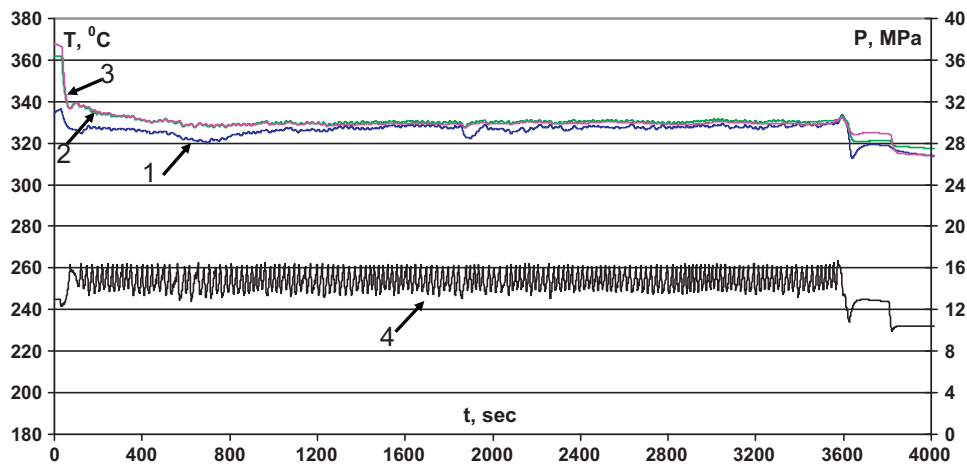


Fig. 5. Reactor temperatures T_{k1} (curve 1), T_{k2} (curve 2), T_{k3} (curve 3) and pressure (curve 4) during operating mode.

oscillations, the LABB remains connected to VI all time while ECG operates thus providing AHFC battery safety.

Thermal energy, which is produced in reactor, is spent on circuit water heating. When circuit water temperature in circuit water tank reaches the fixed value, FH starts. FH intensifies the process of heat transfer to the room. FH is switched off when circuit water temperature drops to respective fixed value.

Today CGPP-10 operating mode duration is limited firstly by the volume of aluminum powder storage bunker. So, now CGPP-10 can nonstop operate during 5 h with hydrogen production rate over $10 \text{ nm}^3 \text{ h}^{-1}$. CGPP-10 stop process (putting into initial state stage) is activated by clicking the stop button on ACMS monitor (Fig. 1).

When stop button is clicked the DHPP is switched from mixing tank to distilled water tank and washes the reactor and respective pipelines. Reactor is washed for 30 s after that DHPP is switched off. 3 min later all oxidation products are totally removed from the reactor. Water is also removed from the condenser, circuit water pump is turned off and CV4 closes.

At the moment when DHPP is turned off FS power supply is switched back from VI to industrial network and LABB is switched off. ECG remains to be loaded only on four steps of BL1. ECG stops when HT pressure drops to initial value. Residual hydrogen is removed from the reactor, from the condenser and from the dehumidifier into the drainage through CV8 after ECG stop.

Putting into initial state stage continues with the following operations: hand valves closing, hotwells emptying, oxidation product receiving tank unloading, mixing tank and oxidation product receiving tank cleaning, hydrogen pipelines and equipment blowing by nitrogen, aluminum powder storage bunker and distilled water tank reloading, LABB charging, experimental data saving, ACMS, ECG control system and FS shutting off.

It is important to remember that CGPP-10 is an experimental plant. Therefore, to provide the safety of CGPP-10 components the experimental procedure includes non-typical for power plant operations such as: hydrogen balloons are initially squeezed by hydrogen, pre-starting operations and putting into initial state stages uses industrial network, LABB remains to be connected to VI all time while ECG operates and others. All of these operations are fail-preventing and should be certainly avoided in power plant marketable versions.

3. Results and discussion

Here “1-h” test results is considered. Although the test is referred to as 1-h, the whole experiment actually lasted more than 1 h. 1 h is the duration of just operating mode, during this time

aluminum–water mixture was being interruptedly injected into the reactor.

The saturated wet steam of water with the initial temperature 330°C and the pressure 13 MPa was created inside the reactor to the end of preliminary reactor heating. First portion of aluminum–water mixture with water to aluminum mass ratio 7.9 was prepared within mixing tank. Aluminum powder with the average particle size of $7 \mu\text{m}$ was used. Three 40 l hydrogen balloons were attached to RB with common initial pressure 2.6 MPa. During the stage of pre-starting operations CGPP-10 consumed 2.7 kWh of electrical energy from industrial network. At the moment when FS was switched from industrial network to LABB (through VI) experimental plant consumed 0.9 kW.

The duration of aluminum–water mixture injection into the reactor in examining test was 1 h. Fig. 5 shows reactor temperatures and pressure. Temperature sensors T_{k1} , T_{k2} , T_{k3} are installed on different reactor height. It is obvious that chemical reactor operated stationary. Variable cross-section valve was programmed to maintain the reactor pressure in the interval of 14–16 MPa. Experimental reactor temperature lay in the interval of $320\text{--}327^\circ\text{C}$. Final temperature and pressure drop in Fig. 5 is connected with the beginning of reactor washing.

During the 1-h test 9.6 kg of aluminum powder and 76 l of water were taken out from aluminum powder storage bunker and distilled water tank, respectively. 9.6 kg of aluminum and 76 l of water came into the mixing tank. But, in the end of test about 2.1 l of aluminum–water mixture remained inside the mixing tank, so it was not used. Therefore, only 9.34 kg of aluminum passed through the reactor. As for water, during the pre-starting operations and the operating mode in total 75 l passed through the reactor.

Experimentally obtained thermodynamic reactor parameters exactly corresponds to the results of computational investigation [19]. Particularly, in accordance with [19] at reactor pressure 15 MPa and water to aluminum mass ratio ($75 \text{ kg}/9.34 \text{ kg}$) ≈ 8 equilibrium reactor temperature should be 324°C . It is seen that theoretical value agrees with an experimental one.

Condenser pressure P_4 and pressure at the entry to HT P_5 are shown in Fig. 6. Fig. 7 shows the following temperatures: condenser gas space T_4 , bottom of condenser body T_5 and circuit water tank T_2 . When condenser pressure increased for the first time to 1 MPa, the initial hydrogen purge was carried out through CV8. Initial purge was finished at $P_4 = 0.6 \text{ MPa}$. When condenser pressure reached 5 MPa, CV7 opened and hydrogen started to feed ECG. Pressure difference between condenser and HT was being created by OWV2. When circuit water tank temperature increased to 53°C , FH was activated. It was deactivated when circuit water tempera-

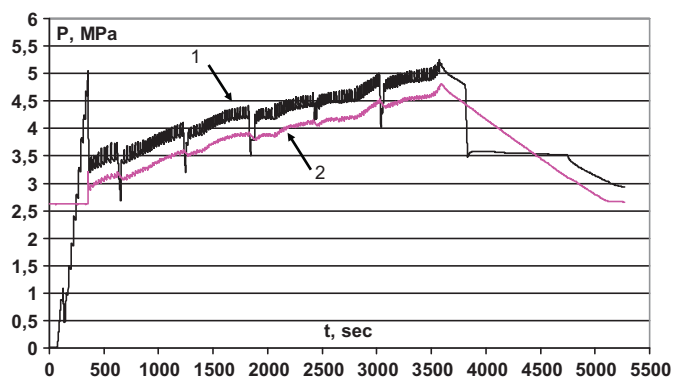


Fig. 6. Condenser pressure P_4 (curve 1) and pressure at the entry to HT P_5 (curve 2) during experiment.

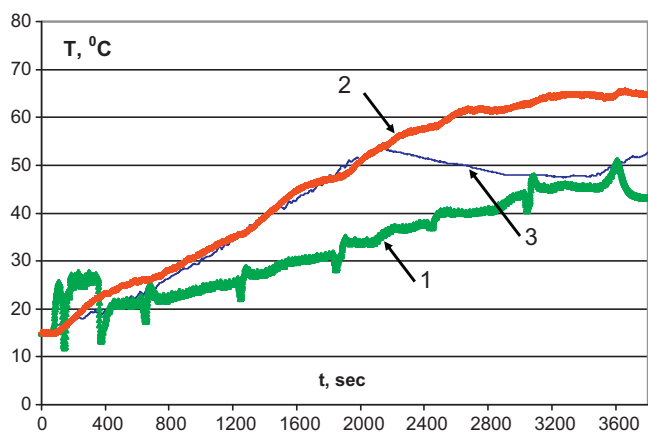


Fig. 7. T_4 – condenser gas space temperature (curve 1), T_5 – bottom of condenser body temperature (curve 2), and T_2 – circuit water tank temperature (curve 3) (during operating mode).

ture decreased to 48 °C. During the 1-h operating mode water was removed from the condenser 5 times. Each removing led to condenser pressure and temperature drop, because with water some hydrogen (dissolved in water and directly in gaseous phase) left the condenser. When DHPP stopped, the residue of water was removed from the condenser as well. Due to the last water removing the condenser pressure fell below HT pressure and it was being less than HT pressure for some time. ECG was consuming the hydrogen from HT and soon the condenser and HT pressures were equalized. ECG stopped when HT pressure reached the initial value of 2.6 MPa. Hydrogen humidity sensor showed that during experiment the dew-point hydrogen temperature did not exceed –25 °C.

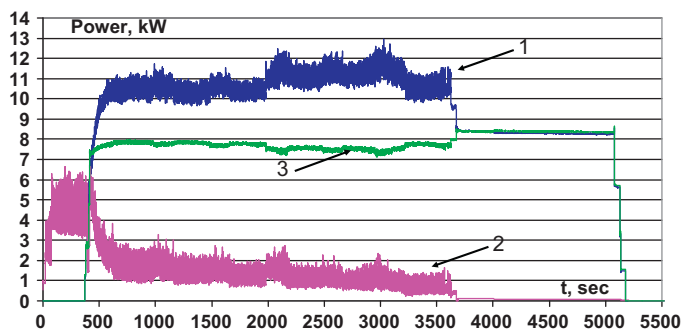


Fig. 8. Power distribution during experiment: curve 1 – produced by ECG, curve 2 – produced by LABB, and curve 3 – consumed by BL1.

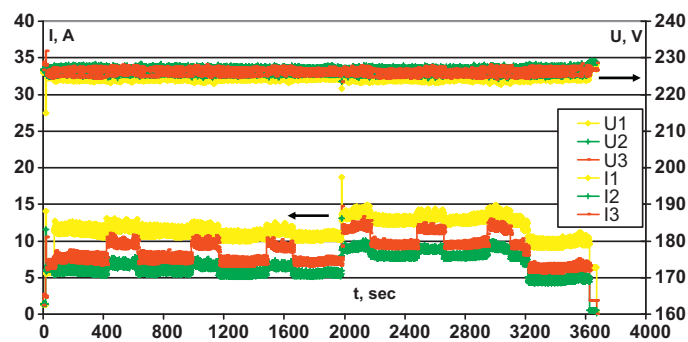


Fig. 9. VI phase currents and voltages during the operating mode.

Fig. 8 shows the power distribution during the experiment. In first minutes of operating mode FS was energized only from LABB. LABB was disconnected from VI just at the end of experiment when DHPP stopped. When DHPP stopped, FS was switched from VI to industrial network, while ECG was remaining to be loaded on four BL1 steps. VI phase currents and voltages are shown in **Fig. 9**. Periodical increases in CGPP-10 power consumption are connected with aluminum dosage screw and water dosage pump periodical runs (mixing tank filling-up). **Fig. 9** shows that during the 1-h test the mixing tank was 6 times refilled. From 1960 to 3200s CGPP-10 power consumption was increased due to FH run.

During the 1-h test the LABB was discharged on 1.5 kWh. BL1, which imitated the DC-power consumer, consumed 10.5 kWh of electrical energy. ECG produced 13.6 kWh (49 MJ) with 38.6% efficiency. Consequently, CGPP-10 auxiliary equipment consumed (from DC-power sources):

$$1.5 \text{ kWh} + 13.6 \text{ kWh} - 10.5 \text{ kWh} = 4.6 \text{ kWh.}$$

ECG consumed:

$$(49 \text{ MJ}/0.386)/142 \text{ MJ kg}^{-1} = 0.893 \text{ kg} (10 \text{ nm}^3) \text{ of hydrogen,}$$

where 142 MJ kg⁻¹ – high heat value of hydrogen.

21.6 kWh (78 MJ) of low-grade heat (~50 °C) was produced in ECG cooling circuit module. Circuit water tank was heating with the average heat rate of 25 kW. The results of test described are gathered in **Table 2**.

The result of solid product X-ray analysis is shown in **Fig. 10**. Presented diffraction spectrum is made of only one crystalline

Table 2
CGPP-10 test results per 1 h of operating mode.

Parameter	Unit	Value
Average reactor pressure	MPa	15
Water to aluminum mass ration within the reactor	–	8
Average reactor temperature	°C	324
Total aluminum consumption	kg	9.6
Useful aluminum consumption (reactor-passed)	kg	9.34
Hydrogen consumption by ECG	nm ³	10
Energy consumption during the stage of pre-starting operations	kWh	2.7
LABB discharge	kWh	1.5
Electrical energy production by ECG	kWh	13.6
Electrical energy consumption by BL1	kWh	10.5
CGPP-10 auxiliary	kWh	4.6
Low-grade heat (50 °C) production by ECG	kWh	21.6
High-grade heat production by RB	kWh	25
Electrical (to aluminum chemical energy) efficiency	%	12
Total (to aluminum chemical energy) efficiency	%	72

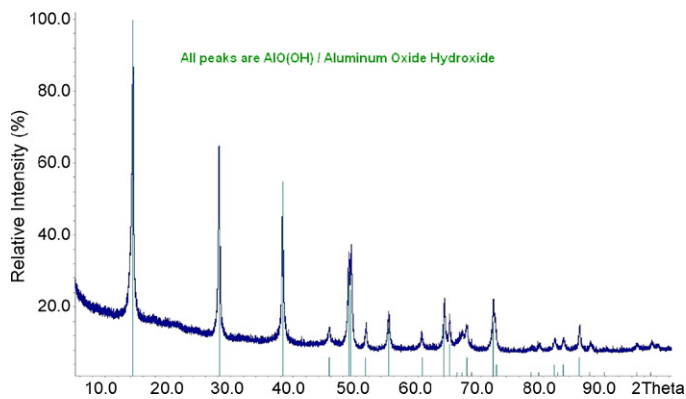


Fig. 10. Solid oxidation product X-ray analysis result.

phase—oxyhydroxide that speaks about high (close to 100%) degree of aluminum conversion and stationarity of nonstop regime.

It is significant to mention that 9.34 kg of aluminum, which passed through the reactor, should give 11.6 nm³ of hydrogen if it is fully oxidized. However, ECG consumed only 10 nm³ during the experiment. This is explained by hydrogen losses due to hydrogen purges at the beginning and at the end of test. It is obvious, that initial and final hydrogen purges will cause smaller relative losses of hydrogen if the duration of power plant operating mode increases.

Electrical energy consumption during the stage of pre-starting operations and residue of aluminum–water mixture in mixing tank will have relatively smaller effect on CGPP-10 technical specifications, if time of CGPP-10 operating mode increases as well. Therefore, electrical and total efficiencies in Table 2 were calculated not-accounting the energy consumption on the stage of pre-starting operations (2.7 kWh). Denominator of electrical and total efficiencies represents the heat value of reactor-passed aluminum:

$$9.34 \text{ kg} \times 8.3 \text{ kWh kg}^{-1} = 77.5 \text{ kWh},$$

where 8.3 kWh kg⁻¹ – heat value (chemical energy) of aluminum.

Numerator of electrical efficiency represents the difference between BL1 consumption and LABB discharge:

$$10.5 \text{ kWh} - 1.5 \text{ kWh} = 9 \text{ kWh}.$$

Numerator of total efficiency represents the sum:

$$9 \text{ kWh} + 25 \text{ kWh} + 21.6 \text{ kWh} = 55.6 \text{ kWh}.$$

Therefore, CGPP-10 electrical efficiency was:

$$\frac{9 \text{ kWh}}{77.5 \text{ kWh}} \approx 12\%.$$

Total efficiency was:

$$\frac{55.6 \text{ kWh}}{77.5 \text{ kWh}} \approx 72\%.$$

No evasion that CGPP-10 has a number of engineering drawbacks. Among them there are non-smoothed DHPP-related current oscillations, different loads on FS phases, range disparity between VI input voltage and ECG output voltage and others. Nevertheless, the main cause of so little electrical efficiency is that reactor-produced thermal energy is not utilized for electrical energy generation. However, aluminum water reaction heat is slightly larger than heat value of produced hydrogen. Moreover, during the oxidation of aluminum the high-temperature and high-pressure mixture of hydrogen and water steam is produced within the reactor. Due to high-grade heat this mixture can be effectively used for electrical energy generation by both modern electrochemical

devices and traditional thermopower plants. But, now in CGPP-10 just a part of hydrogen heat value (about 40%) is converted into electrical energy. Heat energy of aluminum–water reaction is partially transformed into the useful heat warming up the room. An excuse of this circumstance can be the power level. On several kilowatts scale it is hardly to efficiently transform the thermal energy into the electrical energy. Therefore, electrical efficiency increasing is possible only in case of power level increasing. At the same time, it is also necessary to develop and join the additional energy equipment for high-temperature and high-pressure steam–hydrogen mixture utilization with the purpose of electrical energy generation.

4. Some economics

Aluminum and, moreover, aluminum powders represents of course rather expensive fuel for electrical energy generation. Today CGPP-10 consumes industrial aluminum micron-sized powders whose cost starts from 3 \$ kg⁻¹. Since CGPP-10 electrical efficiency is 12%, 1 kg of aluminum gives about 1 kWh of useful electrical energy. Taking into account just fuel component, electrical energy produced by CGPP-10 costs 3 \$ kWh⁻¹. Of course, it is incomparably with stationary grid. But if industrial network is unattainable?

There are a number of cases when stationary grid cannot be used. Among them there are remote deenergized areas, disaster areas, transport plants and others. To solve the energy question in these cases the oil–electrical engines are usually used. And it must be said that the cost of electrical energy produced by oil–electrical engines is not so small. It is determined by the oil price and today it is almost one-order higher than the cost of energy from industrial network as well. Taking the liquid hydrocarbons price as 1 \$ kg⁻¹ [20], the engine efficiency as 30%, the fuel component in electrical energy cost will be 0.3 \$ kWh⁻¹. It is one-order smaller than experimental CGPP-10 (with 12% efficiency) produces now. Of course, aluminum-fueled power plant marketable version should have higher efficiency; and, for instance, 30–40% efficiency will decrease the energy cost up to 0.9–1.2 \$ kWh⁻¹. It will be still several times more than oil-based engine has (taking into account today's aluminum and oil prices). However, it does not induce the flat refusal of aluminum. Sometimes aluminum can be more preferable than liquid hydrocarbons. For example, aluminum-fueled power plant is a sustainable decision for eco-tensity regions, e.g. within megapolises. It can be successfully applied as emergency, military, on-peak power and standby plants. Aluminum–water propulsion is also profitable to be used on submarine or ship [17,21], because in this case seagoing craft takes on its board only fuel (aluminum), while oxidizer (water) is supplied from the outside. To put it briefly, aluminum-fueled power plants can be already used in some special energy fields.

An additional important advantage of aluminum as non-organic fuel is the possibility of its regeneration. The products of aluminum oxidation can be returned to the cycle of aluminum production thus decreasing the cost of aluminum.

5. Conclusion

Aluminum-fueled experimental co-generation power plant CGPP-10 was developed and tested. CGPP-10 nonstop run was organized. The control and management of experimental plant were automated with the help of ACSMS in accordance with the developed and programmed algorithm. CGPP-10 operating mode was organized in autonomous (unconnected from industrial network) regime. Following the results of test CGPP-10 technical specifications and energy indexes were defined.

In operating mode reactor pressure was maintained in fixed range from the interval of 14–16 MPa, water to aluminum mass

ratio was about 8. Average experimental reactor temperature was about 324 °C. CGPP-10 consumed 9.3 kg h⁻¹ of aluminum and produced more than 19 kg h⁻¹ of aluminum hydroxide and 11.6 nm³ h⁻¹ of hydrogen. Produced hydrogen fed ECG. Dew-point temperature of hydrogen did not exceed -25 °C. CGPP-10 outputted 9 kW of electrical power. Auxiliary consumed 4.6 kW. CGPP-10 electrical efficiency was 12% (as compared to aluminum chemical energy). Total efficiency was 72%.

Electrical efficiency of power plants based on aluminum–water reactors can be increased with the development of equipment, which utilizes the high-temperature and high-pressure steam–hydrogen mixture to produce electrical energy. Aluminum-fueled power plants are supposed to be competitive with oil-electrical engines in some special energy fields. Fuel component in electrical energy cost in case of aluminum-fueled power plant is comparable with the cost of electrical energy produced by traditional liquid hydrocarbons. At the same time aluminum-based energy generation is more environmentally friendly.

This work should be continued by the development of improved aluminum-fueled co-generation power plant. Plant should have higher power level, join additional energy equipment for high-temperature and high-pressure steam-hydrogen mixture utilization, be assembled in container and be equipped by easy-to-use control system.

Acknowledgement

Experimental co-generation power plant CGPP-10 was developed and tested due to Financial Support of The Ministry of Education and Science of the Russian Federation. Grant number is 02.526.12.6010.

References

- [1] A. Sheindlin, A. Zhuk, Russian Journal of General Chemistry 77 (2007) 778–782.
- [2] A.Z. Zhuk, A.E. Sheindlin, B.V. Klyemenov, E.I. Shkolnikov, M.Y. Lopatin, Journal of Power Sources 157 (2006) 921–926.
- [3] T. Hiraki, S. Yamauchi, M. Iida, H. Uesugi, T. Akiyama, Environmental Science & Technology 41 (2007) 4454–4457.
- [4] S.S. Martínez, L. Alpañil Sánchez, A.A. Álvarez Gallegos, P.J. Sebastian, International Journal of Hydrogen Energy 32 (2007) 3159–3162.
- [5] E. Shkolnikov, M. Vlaskin, A. Iljukhin, A. Zhuk, A. Sheindlin, Journal of Power Sources 185 (2008) 967–972.
- [6] J.M. Woodall, J.T. Ziebarth, C.R. Allen, D.M. Sherman, J. Jeon, G. Choi, Recent Results on Splitting Water with Aluminum Alloys, John Wiley & Sons Inc., 2008.
- [7] I.L. Kolbenev, Renewable Energy 3 (1993) 227–233.
- [8] S. Yang, H. Knickle, Journal of Power Sources 112 (2002) 162–173.
- [9] Q. Li, N.J. Bjerrum, Journal of Power Sources 110 (2002) 1–10.
- [10] Mineral Commodity Summaries 2010, U.S. Geological Survey, 2010.
- [11] E.C. Partington, International Journal of Production Economics 26 (1992) 211–216.
- [12] Russian Federation Patent 2223221 (in Russian).
- [13] Russian Federation Patent 2278077 (in Russian).
- [14] K. Mahmoodi, B. Alinejad, International Journal of Hydrogen Energy 35 (2010) 5227–5232.
- [15] F. Franzoni, M. Milani, L. Montorsi, V. Golovitchev, International Journal of Hydrogen Energy 35 (2010) 1548–1559.
- [16] S.S. Martínez, W. López Benites, A.A. Álvarez Gallegos, P.J. Sebastián, Solar Energy Materials and Solar Cells 88 (2005) 237–243.
- [17] T.F. Miller, J.L. Walter, D.H. Kiely, Symposium on Autonomous Underwater Vehicle Technology, San Antonio, TX, USA, 2002, pp. 111–119.
- [18] M.S. Vlaskin, E.I. Shkolnikov, A.V. Bersh, International Journal of Hydrogen Energy 36 (2011) 6484–6495.
- [19] M.S. Vlaskin, E.I. Shkolnikov, A.V. Lisicyn, A.V. Bersh, A.Z. Zhuk, International Journal of Hydrogen Energy 35 (2010) 1888–1894.
- [20] Petroleum Marketing Annual 2009, Energy Information Administration, Washington, 2010.
- [21] Russian Federation Patent 2236984 (in Russian).